Journal of Medical Ultrasonics (2023) 50:187–195
https://doi.org/10.1007/s10396-023-01293-z

ORIGINAL ARTICLE–GASTROENTEROLOGY

# Comparison of strain elastography and shear wave elastography in diagnosis of fibrosis in nonalcoholic fatty liver disease

Yu Ogino[1] · Noritaka Wakui[1] · Hidenari Nagai[1] · Takahisa Matsuda[1]

Received: 3 August 2022 / Accepted: 12 January 2023 / Published online: 18 February 2023


## Abstract

**Purpose** To reveal the ability of S-Map strain elastography to diagnose fibrosis in nonalcoholic fatty liver disease (NAFLD) and to compare its diagnostic ability with that of shear wave elastography (SWE).

**Methods** Participants were patients with NAFLD who were scheduled to undergo liver biopsy at our institution between 2015 and 2019. A GE Healthcare LOGIQ E9 ultrasound system was used. For S-Map, the right lobe of the liver was visualized in the section where the heartbeat was detected by right intercostal scanning, a 4 × 2-cm region of interest (ROI) was defined at 5 cm from the liver surface, and ROI strain images were acquired. Measurements were repeated six times, with the average taken as the S-Map value. Correlations of S-Map and SWE values with fibrosis stage determined by liver biopsy were analyzed using multiple comparisons. The diagnostic performance of S-Map for fibrosis staging was assessed using receiver operating characteristic curves.

**Results** In total, 107 patients (65 men, 42 women; mean age 51 ± 14 years) were analyzed. The S-Map value by fibrosis stage was 34.4 ± 10.9 for F0, 32.9 ± 9.1 for F1, 29.5 ± 5.6 for F2, 26.7 ± 6.0 for F3, and 22.8 ± 4.19 for F4. By fibrosis stage, the SWE value was 1.27 ± 0.25 for F0, 1.39 ± 0.20 for F1, 1.59 ± 0.20 for F2, 1.64 ± 0.17 for F3, and 1.88 ± 0.19 for F4. The diagnostic performance of S-Map (measured by area under the curve) was 0.75 for F2, 0.80 for F3, and 0.85 for F4. The diagnostic performance of SWE (measured by area under the curve) was 0.88 for F2, 0.87 for F3, and 0.92 for F4.

**Conclusion** S-Map strain elastography was inferior to SWE in terms of ability to diagnose fibrosis in NAFLD.

**Keywords** Strain elastography · Nonalcoholic fatty liver disease · Ultrasound · Shear wave elastography · Liver stiffness

## Introduction

When treating chronic liver disease, it is important to correctly stage liver fibrosis because the risk of cirrhosis and hepatocellular carcinoma increases as fibrosis progresses [1]. Currently, histopathological evaluation by liver biopsy is considered the gold standard for fibrosis staging [2]. However, liver biopsy cannot be performed repeatedly because it is an invasive procedure that carries risks of bleeding and pain [3]. Various methods for noninvasive staging of fibrosis have been developed and employed. Examples include imaging diagnosis using abdominal ultrasound [4, 5] and abdominal MRI [6–8]; serum markers of fibrosis, such as hyaluronic acid, type IV collagen 7S, and Mac-2 binding protein glycosylation isomer [9–11]; and formulas for estimating liver fibrosis, such as the aspartate aminotransferase (AST) to platelet ratio index (APRI) and fibrosis-4 (FIB-4) index [12, 13].

One method for noninvasive staging of fibrosis is elastography using abdominal ultrasound [14]. There are two approaches to elastography: strain elastography and shear wave elastography (SWE) [15]. The principle of conventional strain elastography techniques (e.g., real-time tissue elastography [RTE]) is to display in color the relative degree of deformation (strain) within a region of interest, achieving qualitative evaluation. On the other hand, S-Map, a strain elastography technique developed by GE Healthcare, enables quantitative evaluation [15]. The principle of S-Map is to directly evaluate and visualize the amounts of strain. The strain measurement closer to the pre-determined maximum strain value is coded in a

✉ Noritaka Wakui
wakui@med.toho-u.ac.jp

[1] Division of Gastroenterology and Hepatology, Department of Internal Medicine (Omori), School of Medicine, Faculty of Medicine, Toho University, 6-11-1 Omori-Nishi, Ota-Ku, Tokyo 143-8541, Japan

warmer color, while a lower strain measurement is coded in a cooler color. There is always a one-to-one relationship between the absolute strain values and the color displayed when the pre-determined scale and external force are unchanged. The quantitative nature of S-Map is a marked difference between it and conventional strain elastography techniques.

Recent studies have described noninvasive methods of fibrosis staging using strain elastography and SWE, but there is still little evidence for their use in nonalcoholic fatty liver disease (NAFLD), including in predicting its prognosis. Furthermore, no studies have yet investigated fibrosis staging in NAFLD using S-Map ultrasound elastography. Therefore, in this study, we aimed to reveal the ability of S-Map ultrasound elastography to diagnose fibrosis in NAFLD and to compare its diagnostic ability with that of SWE.

## Materials and methods

### Enrollment of the participants

Participants were patients with NAFLD who were scheduled to undergo liver biopsy at our institution between 2015 and 2019. Eligibility criteria for study participation were as follows: (1) patient (or family member if the patient is unable to make their own decisions) personally provided written consent to participate, (2) aged 20 years or older, and (3) did not meet other exclusion criteria. NAFLD was diagnosed based on the latest guidelines established by the American Association for the Study of Liver Disease [16] as follows: (i) fatty change of the liver observed by imaging; (ii) no heavy alcohol consumption (ethanol intake < 210 g per week for men and 140 g per week for women); (iii) no other factors inducing fatty change of the liver; and (iv) no chronic liver disease with clear etiology, such as viral infection (hepatitis C virus and B virus), primary biliary cholangitis, or autoimmune hepatitis.

Other exclusion criteria were: (1) narrow intercostal spaces or other issues that would impede liver visualization, (2) pregnant or nursing, (3) ascites, and (4) serious heart disease. Patients with (3) and (4) were excluded because these conditions could affect the results of strain elastography.

The protocols for the prospective study (No. 26-304, M18273; S-Map) and the retrospective study (No. M21217; SWE) were in compliance with the Declaration of Helsinki and were approved by the Ethics Committee of Toho University Omori Medical Center. Information about SWE was published on the website of Toho University Omori Medical Center and patients who opted out were excluded from the study.

### Ultrasonography

Ultrasonography (US) was performed from the right intercostal space using a LOGIQ E9 XDclear (GE Healthcare, Chicago, IL) with a 3.75-MHz convex array probe (C1-6). The mechanical index and frame rate were set to 0.22–0.29 and 15–18 frames/s, respectively. Images showing liver parenchyma of the right hepatic lobe (segment 5) were used in the analysis. Participants were examined in the supine position with the right arm elevated above the head and were instructed to hold their breath. All patients fasted overnight before the examination. All US examinations were performed by an independent examiner who had over 26 years of experience as an ultrasonographer and was blinded to patient characteristics.

### Strain elastography

The S-Map technique developed by GE Healthcare was used for strain elastography. This technique estimates liver stiffness according to the amount of strain in the liver produced by heartbeats. Specifically, the amount of strain is converted to an image, and the color data of the image are quantified. Each pixel is assigned a number that varies from 0 to 100, with the maximum scale (red) being 100 and the minimum scale (blue) 0, as the displayed color moves from cold to warm (Fig. 1). This value is called the "strain index."

Since strain is directly converted to a color image as an absolute value, as long as the scale settings and external force are constant, there is always a one-to-one relationship between the amount of strain and the displayed color.

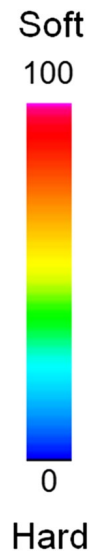


**Fig. 1** Color scale indicating the amount of strain in the liver. Each pixel is assigned a number that varies from 0 to 100 as the displayed color shifts from cold to warm, with the maximum scale (red) set at 100 and the minimum scale (blue) at 0

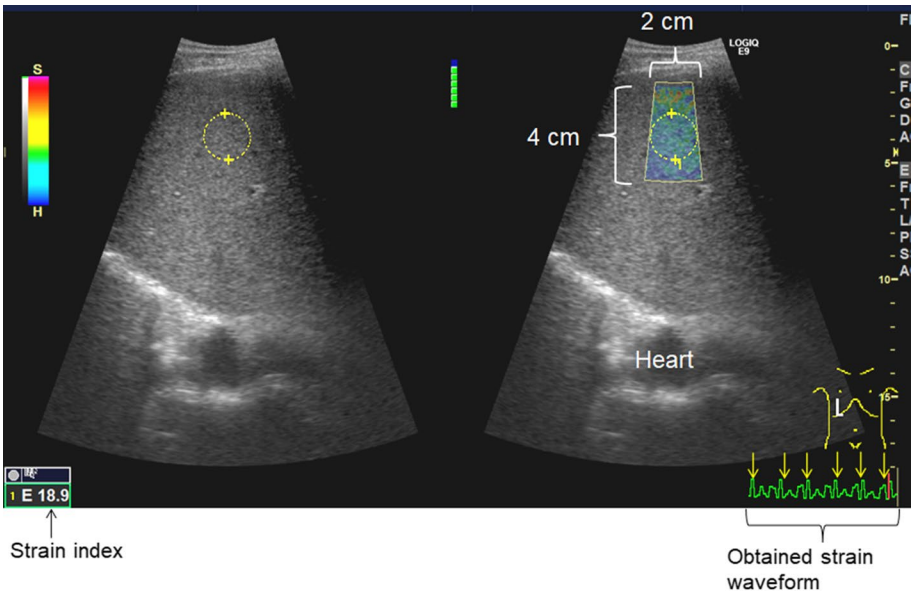


**Fig. 2** Method for S-Map. The section of the right lobe of the liver where the heartbeat was detected was visualized by right intercostal scanning. A 4 × 2 cm region of interest (ROI) was defined at 5 cm from the liver surface and strain images were acquired. The frame of the acquired strain waveform with the greatest strain was selected. A circle was drawn in the ROI to display the strain index. Measurements were repeated a total of six times, and the average value was considered the S-Map value

The actual method used in this study (Fig. 2) is as follows:

1. The right lobe of the liver was visualized using right intercostal scanning in the section where the heartbeat was detected, avoiding blood vessels and other structures of the liver.
2. The S-Map button on the touch panel was pressed to display an ROI 4 cm in length by 2 cm in width, at 5 cm from the liver surface.
3. The patient was asked to hold their breath for approximately 5 s while the strain images were acquired. Measurement was performed using the natural-expiration breath-hold technique in all cases.
4. The frame with the greatest strain in the strain waveform was selected with the trackball as the representative frame (arrow).
5. After the frame was selected, a circle was drawn in the ROI to display the strain index.
6. Measurements were repeated six times, and the average of the obtained values was considered the S-Map value.

## Shear wave elastography (*Fig. 3*)

The following method modeled after a previous study [17] was used:

1. The S5 segment of the liver was visualized by right intercostal scanning. The SWE button on the touch panel was pressed to display an ROI of 3 cm in length by 1.5 cm in width, at 1–2 cm from the liver surface.

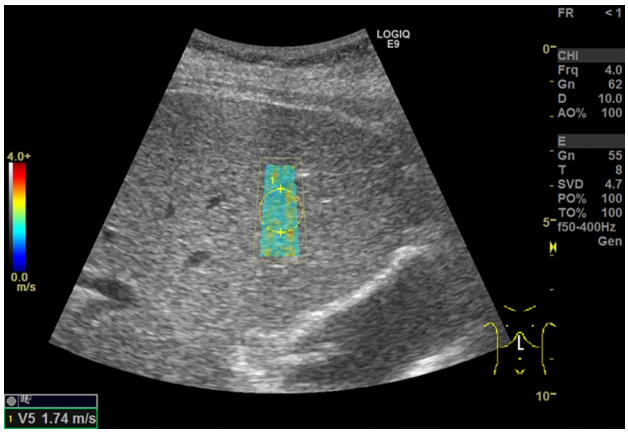


**Fig. 3** Method for shear wave elastography (SWE). The S5 segment of the liver was visualized by right intercostal scanning. A 3 × 1.5 cm region of interest (ROI) was defined at 1–2 cm from the liver surface. The propagation velocity of shear elastic waves in the ROI was measured. Measurements were repeated a total of six times, and the average value was considered the SWE value

2. The patient was asked to hold their breath for approximately 5 s while the propagation velocity of shear elastic waves in the ROI was measured.
3. Measurements were repeated six times, and the average was considered the SWE value.

## Correlation between hematological parameters and liver stiffness

On the same day as ultrasonography, blood tests were performed to measure platelets, albumin, AST, alanine aminotransferase, total bilirubin, prothrombin time,

triglycerides, high-density lipoprotein cholesterol, low-density lipoprotein cholesterol, fasting blood glucose, and hemoglobin A1c. The fibrosis indices APRI and FIB-4 were also calculated, and their correlations with S-Map and SWE values were assessed.

### Diagnostic performance of S-Map and SWE for fibrosis staging

Correlations of S-Map and SWE values with fibrosis stage determined by liver biopsy were analyzed by multiple comparisons. The diagnostic performance of S-Map and SWE values for fibrosis staging was assessed using receiver operating characteristic (ROC) curves and compared against APRI and the FIB-4 index.

### Histopathological examination of the liver

Liver biopsy was performed after sonography with a 16-gauge liver biopsy needle (MISSION Core needle biopsy instrument; Japan Becton Dickinson, Tokyo, Japan). Specimens were obtained from the anterior segment of the right lobe under US guidance and fixed in 10% formalin, embedded in paraffin, and then sectioned and stained with hematoxylin–eosin and azan for histologic evaluation by a single experienced pathologist blinded to the clinical conditions of the patients.

Pathologic liver fibrosis was evaluated using the Clinical Research Network's nonalcoholic steatohepatitis (NASH) scoring system [18], and the diagnosis of NASH was based on the classification described by Matteoni et al. [19].

### Statistical analysis

Continuous variables were tested for a normal distribution. Continuous variables are presented as the mean ± standard deviation or median (interquartile range), as appropriate.

Spearman's rank-order correlation was used to compare the S-Map and SWE values with each factor. Multiple comparisons were made using the Kruskal–Wallis test. ROC analysis was used to calculate the cutoff value and area under the curve (AUC) for liver fibrosis staging. Statistical analysis was performed using BellCurve for Excel 2015 (SSRI Co., Tokyo, Japan). A $p$ value $< 0.05$ was considered to indicate statistical significance.

## Results

### Patients

This study enrolled 114 patients with NAFLD. Seven patients whose specimens were too small to be evaluated or who had a discrepant pathological diagnosis were excluded, leaving 107 patients for analysis. Of these 107 patients, 65 were men and 42 were women, and the mean age was 51 ± 14 years. The fibrosis stage was 0 in 27 patients, 1 in 42 patients, 2 in 11 patients, 3 in 14 patients, and 4 in 13 patients. Activity grade was A0 in nine patients, A1 in 65 patients, A2 in 31 patients, and A3 in two patients. Steatosis grade was S0 in three patients, S1 in 46 patients, S2 in 33 patients, and S3 in 25 patients. Detailed patient characteristics are shown in Tables 1 and 2.

### Correlation between elastography and clinical laboratory parameters

S-Map values were positively correlated with albumin ($r = 0.3058$), platelets ($r = 0.2545$), and prothrombin percentage ($r = 0.2213$), and negatively correlated with AST ($r = -0.2322$), total bilirubin (T-Bil) ($r = -0.2072$), APRI ($r = -0.4141$), and fibrosis-4 (FIB-4) index ($r = -0.2842$).

SWE values were positively correlated with age ($r = 0.4370$), AST ($r = 0.2024$), hemoglobin A1c ($r = 0.1681$), APRI ($r = 0.4522$), and FIB-4 index ($r = 0.5775$), and negatively correlated with albumin

**Table 1** Clinical and biochemical characteristics

| Variables | Value |
|---|---|
| Number | 107 |
| Sex (male/female) | 65/42 |
| Age (years) | 51 ± 14 |
| Body mass index (kg/m$^2$) | 29.0 ± 4.3 |
| AST (IU/L) | 51.3 ± 31.3 |
| ALT (IU/L) | 71.1 ± 45.7 |
| Total bilirubin (mg/dL) | 1.5 ± 0.47 |
| Albumin (g/dL) | 4.2 ± 0.4 |
| Platelet count (× 10$^4$/μL) | 10.7 ± 6.4 |
| Prothrombin time (%) | 71.4 ± 18.2 |
| Triglyceride (mg/dL) | 177.4 ± 102.7 |
| HDL-Chol (mg/dL) | 51.0 ± 12.4 |
| LDL-Chol (mg/dL) | 121.1 ± 34.7 |
| FPG (mg/dL) | 137.4 ± 51.1 |
| HbA1c (%) | 6.7 ± 1.3 |
| APRI | 0.76 ± 0.74 |
| Fib-4 index | 2.09 ± 2.34 |
| S-Map (0–100) | 30.8 ± 9.2 |
| SWE (m/s) | 1.47 ± 0.29 |

Values are expressed as the mean ± standard deviation or number of patients

*ALT* aspartate aminotransferase, *APRI* aspartate aminotransferase to platelet ratio index, *AST* alanine aminotransferase, *FIB-4 index* fibrosis-4 index, *FPG* fasting plasma glucose, *HDL-Chol* high-density lipoprotein cholesterol, *LDL-Chol* low-density lipoprotein cholesterol, *SWE* shear wave elastography

**Table 2** Histological characteristics

| Variables | Value |
|---|---|
| Fibrosis stage (*F*) | 107 |
| F0 | 27 |
| F1 | 42 |
| F2 | 11 |
| F3 | 14 |
| F4 | 13 |
| Activity grade (*A*) | |
| A0 | 9 |
| A1 | 65 |
| A2 | 31 |
| A3 | 2 |
| Steatosis score (*S*) | |
| S0 | 3 |
| S1 | 46 |
| S2 | 33 |
| S3 | 25 |

Values are expressed as the number of patients

**Table 3** Correlation between elastography and clinical/laboratory parameters

| Parameters | S-Map | | SWE | |
|---|---|---|---|---|
| | *r* | *p* | *r* | *p* |
| Age | −0.1600 | 0.1081 | 0.4370 | < 0.001 |
| Sex | 0.0863 | 0.3886 | −0.0980 | 0.3174 |
| Body mass index | −0.2255 | 0.0256 | 0.1496 | 0.1333 |
| AST | −0.2322 | 0.0188 | 0.2024 | 0.0375 |
| ALT | −0.0510 | 0.6107 | −0.0640 | 0.5146 |
| Total bilirubin | −0.2072 | 0.0367 | 0.1762 | 0.0708 |
| Albumin | 0.3058 | 0.0018 | −0.4875 | < 0.001 |
| Platelet count | 0.2545 | 0.0098 | −0.4049 | < 0.001 |
| Prothrombin time | 0.2213 | 0.00261 | −0.5555 | < 0.001 |
| Triglyceride | 0.0394 | 0.6943 | −0.1929 | 0.0476 |
| HDL-Chol | 0.0231 | 0.8287 | −0.0319 | 0.7604 |
| LDL-Chol | 0.1312 | 0.1977 | −0.2054 | 0.0384 |
| FPG | 0.0882 | 0.3779 | 0.0816 | 0.4058 |
| HbA1c | 0.1133 | 0.2618 | 0.1681 | 0.00881 |
| APRI | −0.4141 | < 0.001 | 0.4522 | < 0.001 |
| FIB-4 index | −0.2842 | 0.0038 | 0.5775 | < 0.001 |

*ALT* aspartate aminotransferase, *APRI* aspartate aminotransferase to platelet ratio index, *AST* alanine aminotransferase, *FIB-4 index* fibrosis-4 index, *FPG* fasting plasma glucose, *HDL-Chol* high-density lipoprotein cholesterol, *LDL-Chol* low-density lipoprotein cholesterol, *SWE* shear wave elastography

($r = -0.4875$), platelets ($r = -0.4049$), prothrombin percentage ($r = -0.5555$), TG ($r = -0.1929$), and low-density lipoprotein cholesterol ($r = -0.2054$) (Table 3).

## Comparison of elastography and fibrosis stage

### S-Map by fibrosis stage

The value was $34.4 \pm 10.9$ for F0, $32.9 \pm 9.1$ for F1, $29.5 \pm 5.6$ for F2, $26.7 \pm 6.0$ for F3, and $22.8 \pm 4.19$ for F4. Multiple comparisons showed significant differences between F0 and F3 ($p < 0.05$), F1 and F3 ($p < 0.05$), F0 and F4 ($p < 0.01$), and F1 and F4 ($p < 0.01$).

### SWE by fibrosis stage

The value was $1.27 \pm 0.25$ for F0, $1.39 \pm 0.20$ for F1, $1.59 \pm 0.20$ for F2, $1.64 \pm 0.17$ for F3, and $1.88 \pm 0.19$ for F4. Multiple comparisons showed significant differences between F0 and F1 ($p < 0.05$), F2 and F4 ($p < 0.05$), F3 and F4 ($p < 0.05$), F0 and F2 ($p < 0.01$), F0 and F3 ($p < 0.01$), F0 and F4 ($p < 0.01$), F1 and F3 ($p < 0.01$), and F1 and F4 ($p < 0.01$) (Fig. 4a, b).

## Diagnostic performance of S-Map and SWE for fibrosis staging

### S-Map

For F2 or higher, sensitivity was 71.1%, specificity 69.2%, and AUC 0.75 at a cutoff of 27.4. For F3 or higher, sensitivity was 77.8%, specificity 72.4%, and AUC 0.80 at a cutoff of 27.1. For F4 or higher, sensitivity was 76.9%, specificity 86.7%, and AUC 0.85 at a cutoff of 23.6 (Table 4, Fig. 5).

### SWE

For F2 or higher, sensitivity was 86.8%, specificity 76.5%, and AUC 0.88 at a cutoff of 1.47. For F3 or higher, sensitivity was 77.8%, specificity 78.5%, and AUC 0.87 at a cutoff of 1.58. For F4 or higher, sensitivity was 92.3%, specificity 81.7%, and AUC 0.92 at a cutoff of 1.68 (Table 5, Fig. 6).

### Advanced fibrosis

When F3 or higher was defined as advanced fibrosis and F4 as cirrhosis, the diagnostic performance results (AUC) of S-Map, SWE, APRI, and the FIB-4 index were 0.80, 0.87, 0.80, and 0.85, respectively. AUC results for cirrhosis were 0.85, 0.92, 0.81, and 0.91, respectively (Table 6).

## Discussion

NAFLD is one of the most common chronic liver diseases worldwide [20]. In 1999, Matteoni et al. emphasized the importance of histological diagnosis of NAFLD because

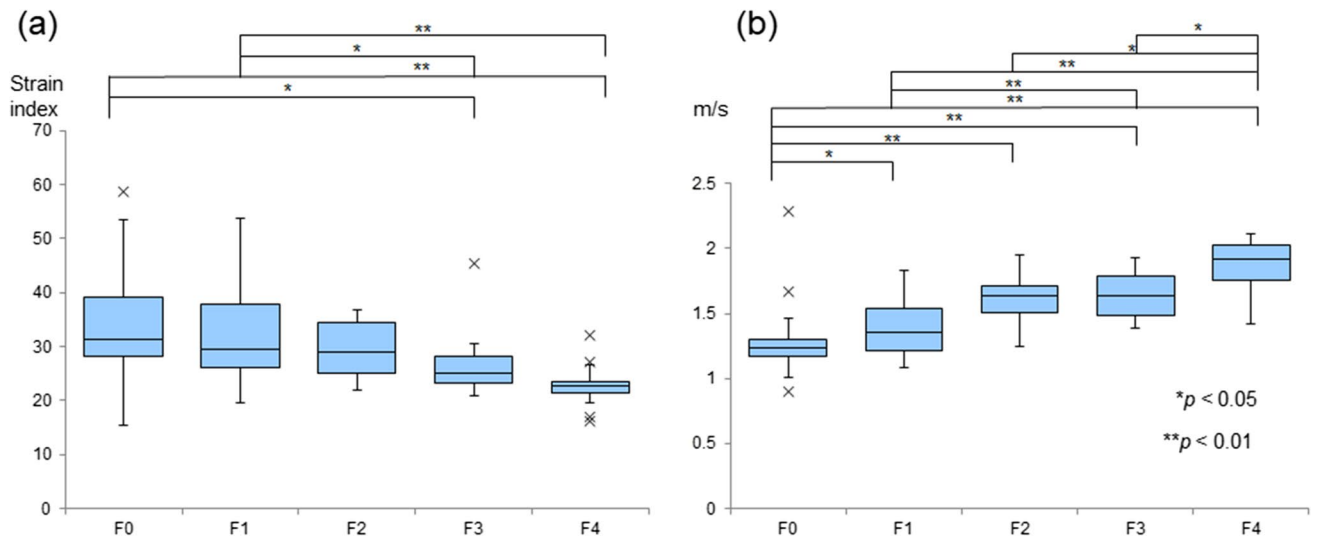


**Fig. 4** **a** Comparison of S-Map value and fibrosis stage. Multiple comparisons showed significant differences between F0 and F3 ($p < 0.05$), F1 and F3 ($p < 0.05$), F0 and F4 ($p < 0.01$), and F1 and F4 ($p < 0.01$). **b** Comparison of shear wave elastography value and fibrosis stage. Multiple comparisons showed significant differences between F0 and F1 ($p < 0.05$), F2 and F4 ($p < 0.05$), F3 and F4 ($p < 0.05$), F0 and F2 ($p < 0.01$), F0 and F3 ($p < 0.01$), F0 and F4 ($p < 0.01$), F1 and F3 ($p < 0.01$), and F1 and F4 ($p < 0.01$)

**Table 4** S-Map value for assessment of histologic fibrosis stage in patients with NAFLD

| | F2 | F3 | F4 |
|---|---|---|---|
| Cutoff value | 27.4 | 27.1 | 23.6 |
| Sensitivity (%) | 71.1 | 77.8 | 76.9 |
| Specificity (%) | 69.2 | 72.4 | 86.7 |
| AUC curve | 0.75 | 0.80 | 0.85 |

*AUC* area under the curve, *F* fibrosis stage, *NAFLD* nonalcoholic fatty liver disease

NASH with histological findings of ballooning degeneration has a poor prognosis [19]. However, large epidemiological studies from 2015 and later have concluded that liver fibrosis is what determines the prognosis of NAFLD patients [21, 22]. Presently, fibrosis stage is considered more important than whether or not a patient has NASH. Patients with advanced fibrosis (stages 3 and 4) have a particularly poor prognosis, and this has come to be called advanced fibrotic NAFLD [22]. By 2030, the prevalence of NAFLD in Japan is expected to rise to well over 20 million patients, and the

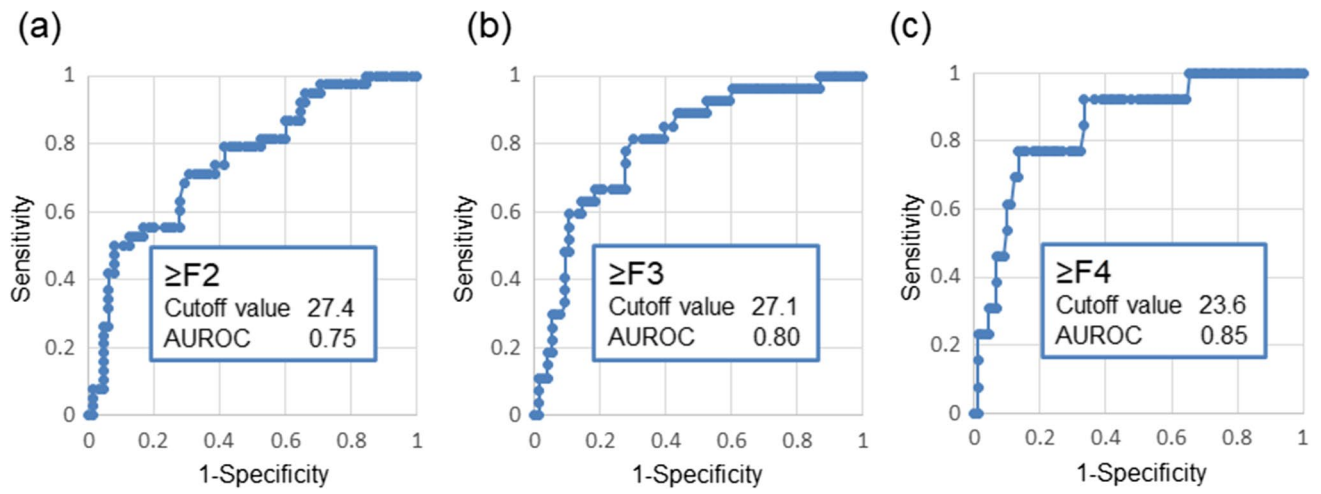


**Fig. 5** Performance of S-Map values for staging fibrosis. **a** The area under the receiver operating characteristic (AUROC) for F2 or higher was 0.75. **b** The AUROC for F3 or higher was 0.80. **c** The AUROC for F4 or higher was 0.85

**Table 5** SWE value for assessment of histologic fibrosis stage in patients with NAFLD

| | F2 | F3 | F4 |
|---|---|---|---|
| Cutoff value (m/s) | 1.47 | 1.58 | 1.68 |
| Sensitivity (%) | 86.8 | 77.8 | 92.3 |
| Specificity (%) | 76.5 | 78.5 | 81.7 |
| AUC curve | 0.88 | 0.87 | 0.92 |

*AUC* area under the curve, *F* fibrosis stage, *NAFLD* nonalcoholic fatty liver disease, *SWE* shear wave elastography

prevalence of advanced fibrotic NAFLD (with stage 3–4 fibrosis) is expected to increase to over 1 million patients [23]. The challenge is how to identify these advanced fibrotic NAFLD patients. Although liver biopsy is considered the gold standard for staging fibrosis, it is invasive and has a problematic rate of sampling errors. Therefore, there is an urgent need to develop a noninvasive test for NAFLD.

Ultrasound elastography, a noninvasive method for diagnosing liver fibrosis, has been demonstrated to be useful for fibrosis staging in various liver diseases. However, few studies have investigated its utility in NAFLD, and most of them have been small studies [24–28]. Furthermore, no study has yet investigated fibrosis staging in NAFLD using the S-Map ultrasound elastography technique. Therefore, in this study, we investigated the diagnostic performance of S-MAP for fibrosis staging in NAFLD. The performance (AUC) of this technique for staging fibrosis at F2 and higher, F3 and higher, and F4 was 0.75, 0.80, and 0.85, respectively.

To date, the diagnostic performance of strain elastography for fibrosis staging in NAFLD has been investigated for only RTE. Orlacchio et al. performed RTE in 52 patients with NASH and reported AUCs of 0.86 and 0.92 for staging fibrosis at F0 and higher and F2 and higher [29]. Ochi et al. also performed RTE in 75 patients with NAFLD and reported AUCs of 0.84, 0.85, 0.88, and 0.97 for staging fibrosis at F1 and higher, F2 and higher, F3 and higher, and F4 [30]. However, the difference between the two techniques is that RTE measures the relative amount of strain, whereas S-Map measures the absolute amount of strain. Therefore, it is important to note that the performance of RTE and S-Map cannot be directly compared, because they have different principles, even though they are both strain elastography techniques.

Other elastography techniques have also been studied. Cassinotto et al. reported the diagnostic performance of SuperSonic Imagine's SWE, Echosens' transient elastography (TE), and Siemens' acoustic radiation force impulse (ARFI) elastography in 91 patients with NAFLD [31]. AUCs of SWE for F2 and higher, F3 and higher, and F4 were 0.86, 089, and 0.88, respectively. AUCs of TE for F2 and higher, F3 and higher, and F4 were 0.82, 0.86, and 0.87, respectively. AUCs of ARFI for F2 and higher, F3 and higher, and

**Table 6** AUC curve of histologic fibrosis stage in patients with NAFLD

| AUC curve | F3/4 (advanced fibrosis) | F4 (liver cirrhosis) |
|---|---|---|
| S-Map | 0.80 | 0.85 |
| SWE | 0.87 | 0.92 |
| APRI | 0.80 | 0.81 |
| FIB-4 index | 0.85 | 0.91 |

*APRI* aspartate aminotransferase to platelet ratio index, *AUC* area under the curve, *F* fibrosis stage, *FIB-4 index* fibrosis-4 index, *NAFLD* nonalcoholic fatty liver disease, *SWE* shear wave elastography

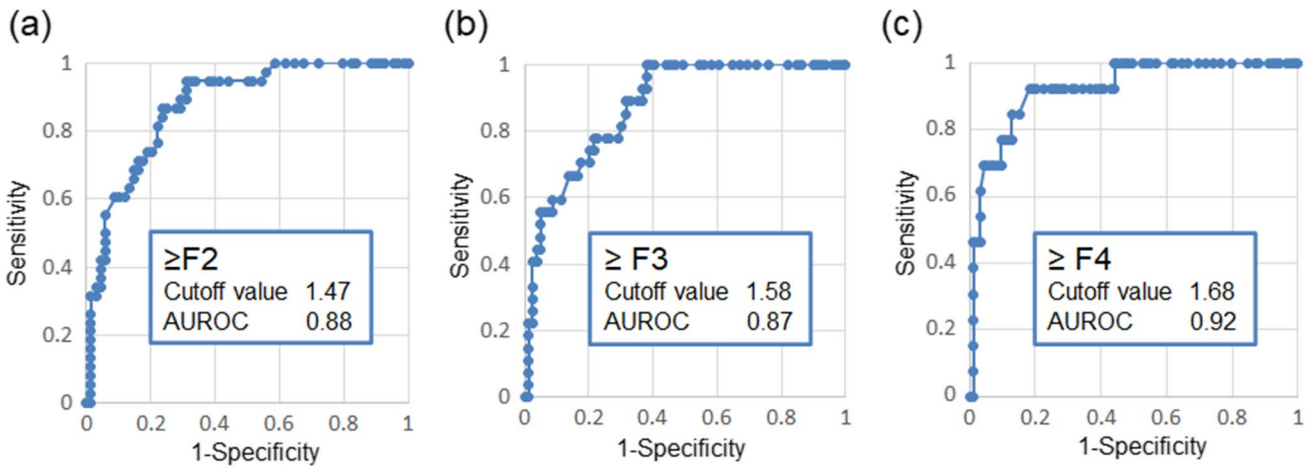


**Fig. 6** Performance of SWE values for staging fibrosis. **a** The area under the receiver operating characteristic (AUROC) for F2 or higher was 0.88. **b** The AUROC for F3 or higher was 0.87. **c** The AUROC for F4 or higher was 0.92

F4 were 0.77, 0.84, and 0.84, respectively. In addition, a study of 54 patients with NAFLD conducted by Furlan et al. assessed the fibrosis-staging performance of GE Healthcare's SWE mode [32], the same one that we investigated in this study. In their study, the AUC of SWE for significant fibrosis (≥F2) was 0.80, and that for advanced fibrosis (≥F3) was 0.89. In our study, the AUCs of GE Healthcare's SWE for F2 and higher, F3 and higher, and F4 fibrosis were 0.88, 0.87, and 0.92, respectively, which were comparable to the previous results described above.

Next, we will discuss results regarding staging performance for advanced fibrotic NAFLD, meaning F3 or higher and F4 fibrosis. AUCs for F3 or higher and F4 were 0.80 and 0.85 for S-Map, 0.87 and 0.92 for SWE, 0.80 and 0.81 for APRI, and 0.85 and 0.91 for FIB-4 index. SWE had the best staging performance for both F3 and higher and F4 fibrosis. Elastography that uses abdominal ultrasound is noninvasive and can be performed repeatedly to assess fibrosis, which is an advantage over methods using FIB-4 index and APRI involving slightly invasive blood tests. Another advantage of elastography is that screening for hepatocellular carcinomas can be performed along with fibrosis staging as both can be performed using abdominal ultrasound. Factors that could explain why S-Map did not perform as well as SWE are the effects of liver inflammation and cholestasis. AST and T-Bil were hematological parameters that were significantly correlated with S-Map. S-Map was significantly correlated with T-Bil, but SWE was not. This suggests that cholestasis, as expressed by T-Bil, could partially explain the poorer diagnostic performance of S-Map. Both S-Map and SWE were significantly correlated with AST, but S-Map had a higher correlation coefficient (r), indicating that S-Map may be more strongly influenced by liver inflammation than SWE. Based on the above findings, S-Map was inferior to SWE in terms of ability to diagnose fibrosis in NAFLD, but it was more sensitive to cholestasis and liver inflammation compared with SWE. Thus, the usefulness of S-Map may well be found when it is used for assessment and follow-up observation in cholestatic diseases (e.g., primary biliary cholangitis and drug-induced liver injury), or for assessment of exacerbation risk and follow-up observation in acute hepatitis.

Another reason for the difference in diagnostic performance might be the major difference in the principles of these two types of elastography, i.e., SWE measures the velocity of shear waves, whereas strain elastography measures strain in the liver. However, further investigation on this topic is needed.

One limitation of this study is that S-Map may not produce accurate results in patients with ascites or heart disease because it is a heartbeat-based technique, and we, therefore, were unable to use the technique in such patients. Other limitations are that our study was conducted at a single institution and in only one ethnic group. Further research at multiple institutions and in multiple ethnic groups is warranted.

## Conclusion

This study revealed the ability of S-Map ultrasound elastography to diagnose fibrosis in NAFLD. S-Map ultrasound elastography was inferior to SWE in terms of ability to diagnose fibrosis in NAFLD.

**Acknowledgements** We thank Shunichirou Tanigawa, Takuma Oguri, and Naohisa Kamiyama for providing advice on the S-Map strain elastography technique.

**Data availability** The datasets generated and/or analyzed during the current study are available from the corresponding author on reasonable request.

## Declarations

**Conflict of interest** YO, NW, HN, and TM declare that they have no conflicts of interest.

**Ethical approval** All the procedures followed were in accordance with the ethical standards of the responsible committee on human experimentation (institutional and national) and with the Helsinki Declaration of 1964 and later versions. This study was approved by the Ethics Committee of Toho University Omori Medical Center.

## References

1. National Institutes of Health Consensus Development Conference Statement. Management of hepatitis C 2002 (June 10–12, 2002). Gastroenterology. 2002;123:2082–99.
2. Castera L. Noninvasive methods to assess liver disease in patients with hepatitis B or C. Gastroenterology. 2012;142:1293–302.
3. Cadranel JF. Good clinical practice guidelines for fine needle aspiration biopsy of the liver: past, present and future. Gastroenterol Clin Biol. 2002;26:823–4.
4. Wakui N, Takayama R, Kanekawa T, et al. Usefulness of arrival time parametric imaging in evaluating the degree of liver disease progression in chronic hepatitis C infection. J Ultrasound Med. 2012;31:373–82.
5. Wakui N, Nagai H, Yoshimine N, et al. Flash imaging used in the post-vascular phase of contrast-enhanced ultrasonography is useful for assessing the progression in patients with hepatitis C virus-related liver disease. Ultrasound Med Biol. 2019;45:1654–62.
6. Mariappan YK, Glaser KJ, Ehman RL. Magnetic resonance elastography: a review. Clin Anat. 2010;23:497–511.
7. Glaser KJ, Manduca A, Ehman RL. Review of MR elastography applications and recent developments. J Magn Reson Imaging. 2012;36:757–74.
8. Igarashi H, Shigiyama F, Wakui N, et al. Whole hepatic lipid volume quantification and color mapping by multi-slice and multi-point magnetic resonance imaging. Hepatol Res. 2019;49:1374–85.
9. Wong VS, Hughes V, Trull A, et al. Serum hyaluronic acid is a useful marker of liver fibrosis in chronic hepatitis C virus infection. J Viral Hepat. 1998;5:187–92.

10. Rockey DC, Bissel DM. Noninvasive measures of liver fibrosis. Hepatology. 2006;43:113–20.
11. Yamada N, Sanada Y, Tashiro M, et al. Serum Mac-2 binding protein glycosylation isomer predicts grade F4 liver fibrosis in patients with biliary atresia. J Gastroenterol. 2017;52:245–52.
12. Wai CT, Greenson JK, Fontana RJ, et al. A simple noninvasive index can predict both significant fibrosis and cirrhosis in patients with chronic hepatitis C. Hepatology. 2003;8:518–26.
13. Vallet-Pichard A, Mallet V, Nalpas B, et al. FIB-4: an inexpensive and accurate marker of fibrosis in HCV infection. Comparison with liver biopsy and fibrotest. Hepatology. 2007;46:32–6.
14. Ferraioli G, Filice C, Castera L, et al. WFUMB guidelines and recommendations for clinical use of ultrasound elastography: Part 3: liver. Ultrasound Med Biol. 2015;41:1161–79.
15. Kudo M, Shiina T, Moriyasu F, et al. JSUM ultrasound elastography practice guidelines: liver. J Med Ultrason. 2013;40:325–57.
16. Chalasani N, Younossi Z, Lavine JE, et al. The diagnosis and management of nonalcoholic fatty liver disease: practice guidance from the American association for the study of liver disease. Hepatology. 2018;67:328–57.
17. Abe T, Kuroda H, Fujiwara Y, et al. Accuracy of 2D shear wave elastography in the diagnosis of liver fibrosis in patients with chronic hepatitis C. J Clin Ultrasound. 2018;46:319–27.
18. Kleiner DE, Brunt EM, Van Natta M, et al. Design and validation of a histological scoring system for nonalcoholic fatty liver disease. Hepatology. 2005;41:1313–21.
19. Matteoni CA, Younossi ZM, Gramlich T, et al. Nonalcoholic fatty liver disease: a spectrum of clinical and pathological severity. Gastroenterology. 1999;116:1413–9.
20. Petta S, Muratore C, Craxi A. Non-alcoholic fatty liver disease pathogenesis: the present and the future. Dig Liver Dis. 2009;41:615–25.
21. Angulo P, Kleiner DE, Dam-Larsen S, et al. Liver fibrosis, but no other histologic features, is associated with long-term outcomes off patients with nonalcoholic fatty liver disease. Gastroenterology. 2015;149:389-97.e10.
22. Hagström H, Nasr P, Ekstedt M, et al. Fibrosis stage but not NASH predicts mortality and time to development of severe liver disease in biopsy-proven NAFLD. J Hepatol. 2017;67:1265–73.
23. Estes C, Anstee QM, Arias-Loste MT, et al. Modeling NAFLD disease burden in China, France, Germany, Italy, Japan, Spain, United Kingdom, and United States for the period 2016–2030. J Hepatol. 2018;69:896–904.
24. Yoneda M, Thomas E, Sclair SN, et al. Supersonic shear imaging and transient elastography with the XL probe accurately detect fibrosis in overweight or obese patients with chronic liver disease. Clin Gastroenterol Hepatol. 2015;13:1502-9.e5.
25. Gaia S, Carenzi S, Barilli AL, et al. Reliability of transient elastography for the detection of fibrosis in non-alcoholic fatty liver disease and chronic viral hepatitis. J Hepatol. 2011;54:64–71.
26. Petta S, Di Marco V, Cammà C, et al. Reliability of liver stiffness measurement in non-alcoholic fatty liver disease: the effects of body mass index. Aliment Pharmacol Ther. 2011;33:1350–60.
27. Wong VWS, Vergniol J, Wong GLH, et al. Diagnosis of fibrosis and cirrhosis using liver stiffness measurement in nonalcoholic fatty liver disease. Hepatology. 2010;51:454–62.
28. Yoneda M, Yoneda M, Mawatari H, et al. Noninvasive assessment of liver fibrosis by measurement of stiffness in patients with nonalcoholic fatty liver disease (NAFLD). Dig Liver Dis. 2008;40:371–8.
29. Orlacchio A, Bolacchi F, Antonicoli M, et al. Liver elasticity in NASH patients evaluated with Real-time elastography (RTE). Ultrasound Med Biol. 2012;38:537–44.
30. Ochi H, Hirooka M, Koizumi Y, et al. Real-time tissue elastography for evaluation of hepatic fibrosis and portal hypertension in nonalcoholic fatty liver fibrosis. Hepatology. 2012;56:1271–8.
31. Cassinotto C, Boursier J, de Lédinghen V, et al. Liver stiffness in nonalcoholic fatty liver disease: a comparison of supersonic shear imaging, FibroScan, and ARFI with liver biopsy. Hepatology. 2016;63:1817–27.
32. Furlan A, Tublin ME, Yu L, et al. Comparison of 2D shear wave elastography, transient elastography, and MR elastography for the diagnosis of fibrosis in patients with nonalcoholic fatty liver disease. AJR Am J Roentgenol. 2020;214:W20–6.